International Journal of Industrial Electronics, Control and Optimization © 2018 IECO

Vol. 1, No. 1, pp. 61-70, June (2018)

Adaptive Gain Scheduling Control of Doubly Fed Induction Generator Based Wind Turbines to Improve Fault Ride Through Performance

Ahmad Khajeh[a] and **Zahra Shabani**[b]

ABSTRACT

The Doubly-Fed Induction Generators (DFIG) based Wind Turbines (WT) are widely used in WTs connected to power systems. Traditionally the back-to-back converters are used in order to control the DFIG. In this paper, an Indirect Matrix Converter (IMC) is utilized. Compared with back-to-back converters, IMCs have numerous advantages such as: higher level of robustness, reliability, reduced size and weight due to the absence of bulky electrolytic capacitor. According to the recent grid codes it is required that wind turbines remain connected to the grid during grid faults. It means that the plant must be in operation and be able to tolerate the fault conditions. This feature is called Fault Ride-Through (FRT) capability of wind plants. To improve FRT capability of the wind turbine, in this paper an adaptive gain scheduling controller is proposed. The proposed method could increase the damping of fault currents and hence attribute more time to controller for reactive power injection. Therefore, the new FRT standards are satisfied. PSIM simulation results confirm the efficiency of the proposed method.

ARTICLE INFO

Keywords:
DFIG
FRT
Indirect matrix converter
Wind turbine
Article history:
Received February. 26, 2018
Accepted Aprill. 11, 2018

I. INTRODUCTION

Due to their superior characteristics, most of the grid-connected WTs operate at a variable speed. Among the different variable speed types, the DFIG is the most promising one[1]. The basic configuration of a WT based on the DFIG is shown in Fig 1. The stator winding of DFIG is directly connected to the grid, while the rotor winding is connected to the grid through an ac-ac power electronic converter having bidirectional switches. Traditionally the back-to-back converters are used to excite the rotor circuit of DFIG. The presence of dc-link capacitor in this arrangement is a serious drawback as increases the costs and reduces the overall lifetime of the system and also makes the system bulky[2].

In this paper, the back-to-back converter arrangement is replaced by an indirect matrix converter (IMC) to control the generator. The main advantages of a matrix converter are: robustness, reliability with less size and weight due to the absence of the bulky electrolytic capacitor, controllable input power factor, nearly sinusoidal input current and output voltage with only switching frequency harmonics, along with bidirectional power flow. The direct matrix converter (DMC) encounters the commutation problems requiring a complex control circuitry. While in IMC all switches at the line side will turn on and off at zero current, so the commutation problems are eliminated[3]. Therefore, the IMCs are the most promising devices for wind energy applications regarding their robustness, reduced size and reliability concerns.

In the past, based on most grid codes, wind turbines were allowed to be disconnected from the grid during the grid disturbance and abnormal voltage reduction. With the increased capacity of wind powers in the power systems over the years, a sudden loss of wind turbines during the grid faults resulting from turbines disconnection could generate control problems of frequency and voltage in the system so leading to the voltage collapse in worst case. The increased penetration of wind energy into the power system over the last decade has therefore led to a serious concern about its influence on the dynamic behavior of the power system. To handle this issue the grid codes are revised by system operators in several countries[4]. According to the new grid codes the wind turbines must be remain connected to the network on the occurrence of grid fault and tolerate the resulting voltage drops. This feature is known as the fault ride-through (FRT) capability of a power plant. The FRT requirement defines that the grid voltage can be how long and how deep at which the wind turbines are allowed to be disconnected from grid. Moreover, in some grid codes such as Germany, wind turbines should also inject reactive power to help the grid voltage recovery.

Because of direct connection of stator winding to the grid and the small rating of power electronic converter in the rotor side, DFIG based wind turbine is very sensitive to grid disturbances, especially to voltage dips during grid faults. Grid faults, even those occurring far from

[a] Corresponding Author: akhajeh@ece.usb.ac.ir, Tel: +82-2-554-0185, Fax: +82-2-554-0186, Faculty of Electrical and Computer Engineering, University of Sistan and Baluchestan, Zahedan, Iran
[b] zshabani@math.usb.ac.ir, Department of Mathematics, Faculty of Mathematics, University of Sistan and Baluchestan, Zahedan, Iran
http://dx.doi.org/10.22111/ieco.2018.24173.1012

the wind turbines, can cause voltage drops at the point of wind turbine connection. The abrupt drop of the grid voltage will make an increase in the current of stator windings of the DFIG. Because of the magnetic coupling between stator and rotor, this current will also flow in the rotor circuit and the power converter. At present, the back-to-back converter is the most frequently used power electronic converter in the wind turbines industry. Therefore, the most of research works have been done to enhance the FRT ability of DFIG utilizing this type of converters. So the grid faults cause over current in the rotor windings and over voltage in the dc-link capacitor hence the proper protection should be provided to safekeeping the converter. Various solutions have been proposed to solve the problem. Some of them are briefly reviewed as follows.

The most popular and reliable method is based on the use of a protective circuit known as crowbar. The crowbar consists of resistors connected to the rotor windings by means of electronic switches. In active crowbar the switches are controllable such as IGBTs whereas in passive one they are anti parallel thyristors. The active crowbar allows opening the circuit when the currents reach to safe region. The passive crowbar allows closing the circuit but not to open it until the crowbar currents reach to zero. Therefore, according to the new grid codes, the passive crowbar is not appropriate for the modern wind turbines. When a fault occurs, the rotor windings get connected to the crowbar while the converter is tripped. Several papers have discussed the implementation and control of crowbar[5–11]. The crowbar can effectively protect the rotor converter under serious grid faults. But its main drawback is that, when the crowbar is activated, the rotor converter cannot control the active and reactive power during crowbar activation so, the DFIG operates as a cage induction generator, absorbing extra reactive power from the grid and deteriorates the grid voltage profile.

Another approach is to modify the rotor-side converter control system to limit the fault currents without using any extra hardware circuit[12–19]. In this method at serious grid faults, the required voltage in the rotor-side converter becomes too large and exceeds its voltage capability. Therefore, the rotor current greatly increases thus leading to converter destruction. This method is beneficial as it does not require any additional hardware but applicable only for moderate faults.

Another solution for FRT is to use an additional energy storage system (ESS) connected to the dc-link[20–23]. The ESS can balance the extra power that goes through the rotor circuit during a grid fault transient, but it also requires a rotor side converter with higher current ratings having extra cost and more system complexity.

Utilizing matrix converters in DFIG wind turbines is still in research phase. Most of the works have dealt with their normal operation. Sigma-delta modulator to control IMC switches of DFIG based WT is proposed in[24]. By using this modulation method, torque pulsations and harmonic content of currents are reduced. Therefore, the power quality of WT is improved. The capability of the input converter to generate different virtual dc-link voltage levels is also proposed in[25]. This method reduces both the commutation losses of output converter and common mode voltage. Due to small voltage required around the synchronous speed, this strategy is applicable in DFIG applications.

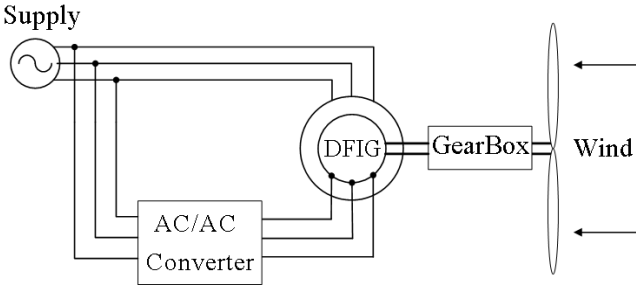

FIG. 1. Wind turbine based on the DFIG.

Dynamic performance of DFIG using two-stage IMC under voltage dip condition has been discussed in[26] without providing any protection. As simulation results show for 80% terminal voltage sag, the stator current reaches to 2.5 pu. Without any protection method, this high current can damage the IGBT switches of the IMC. According to new FRT standards it is required the reactive power to be injected to improve the recovery of voltage during and after grid faults. Results of[26] indicate that, during the fault, about 0.7 pu reactive power is absorbed from the grid which make the voltage deeper. Therefore, the existing controller which is designed for normal operating condition is ineffective during fault conditions.

To solve these drawbacks and satisfy the new FRT standards, in present paper a new method is proposed to protect the IMC with DFIG following the grid faults. In this method an adaptive controller (instead of conventional PI controller) is designed. The proposed method increases the damping of rotor currents. So, the reactive power injection is achieved faster and the new FRT standard is well satisfied. The PSIM simulation results confirm the efficiency of the proposed method.

II. FRT REQUIREMENT

The German transmission system operator E.ON Netz was the first power system operator, who introduced grid codes for wind turbines and is followed now by many other network operators in several countries. E.ON introduces a voltage profile, the limiting curves and regions defining the FRT requirement as shown in Fig. 2 Accordingly, wind turbines must stay connected even when the voltage at the point of common coupling (PCC) of the grid drops to zero. The 150 ms delay shown in Fig. 2 accounts for the normal operating time of protection relays. Three-phase short circuits or fault-related symmetrical voltage dips must not lead to instability above the limit

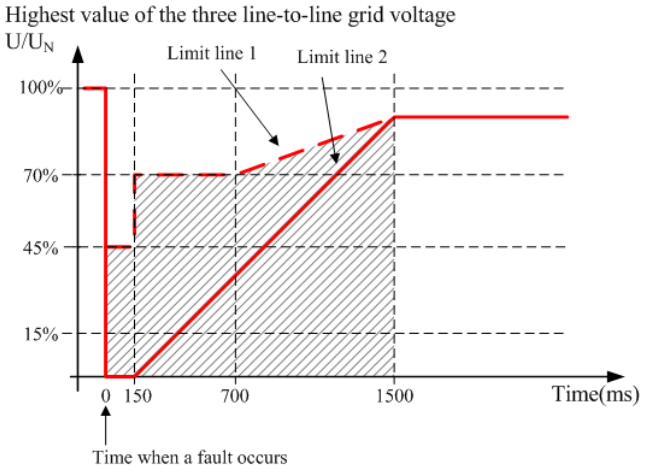

FIG. 2. E. ON Netz LVRT requirement.

line 1 in Fig. 2 or disconnection of the wind turbines from the grid. Within the shaded area and above limit line 2 in Fig. 2, FRT is also required but in case of instability a short term interruption (STI) is allowed. Below the limit line 2 in Fig. 2, no FRT is required and STI from the grid is always permissible. Here, resynchronization times of more than 2 seconds and an active power increase following fault clearance of less than 10% of the rated power per second are also possible. According to the E.ON Netz grid code, wind turbines have to provide a mandatory voltage support during voltage dips. Wind turbines have to supply 1 pu reactive current when the voltage falls below 0.5 pu.

III. MODELING AND CONTROL OF DFIG BASED WIND TURBINE

In this section, dynamics model of both electrical and mechanical parts of DFIG based wind turbine is provided. The stator winding of DFIG is directly connected to the grid, and the rotor winding is coupled via an IMC. The IMC must handle the slip power, i.e. about 30% of the rated power of wind turbine. The speed range of the generator is typically of synchronous speed, thus providing flexibility to operate in both sub and super synchronous modes, depending on the wind conditions. The inverter of the IMC is used to control the active and reactive power of the DFIG. The rectifier of the IMC is often operated at unity power factor. Depending on the rotor speed, the IMC will either absorb power (sub-synchronous) from grid or inject power (super-synchronous) to the grid. Therefore, the IMC must have the ability of bidirectional power flow to the network.

A. Turbine model

The mechanical power extracted by a wind turbine from the wind is expressed by

$$P = \frac{1}{2} A.\rho.C_p(\lambda,\beta).v_w^3 \tag{1}$$

where A is the area covered by the rotor blades, ρ is the air density, C_p is the power coefficient, representing the amount of power the turbine can extract, and vw is the wind speed. The power available in the wind cannot be extracted completely. Theoretically the maximum captured power is 59% of the power available in the wind. The power coefficient is a function of the tip-speed ratio λ and the pitch angle of the rotor blades β. The tip-speed ratio is defined by

$$\lambda = \frac{R\Omega_t}{v_w} \tag{2}$$

Where R is the radius of the rotor blades and Ω_t is the angular speed of the blades. For each pitch angle of the rotor blades, there is an optimum tip-speed ratio λ_{opt} for which $C_p(\lambda_{opt},\beta)$ takes a maximum value.

B. Drive train

Despite of the complexity of the drive train system in a real wind power plant, the dynamic model is reduced to a two- mass system. To assess the dynamic behavior the drive train needs to be considered. For modeling the drive train knowledge of gear transmission ratio, the stiffness c and the damping coefficient d of the shaft is required. The drive train system is described by

$$\begin{aligned} T_R &= J_R.\tfrac{d\Omega_R}{dt} + (\Omega_R - \Omega_G).d + (\theta_R - \theta_G).c \\ T_G &= -J_G.\tfrac{d\Omega_G}{dt} + (\Omega_R - \Omega_G).d + (\theta_R - \theta_G).c \\ \Omega_G &= G\Omega_R \end{aligned} \tag{3}$$

Where T is torque, J is moment of inertia, Ω is angular speed, and γ is angle. Subscripts R and G represent rotor and generator side respectively.

C. DFIG model

For DFIG modeling a fifth-order dynamic model of the DFIG is used in this paper. The model in a two-axis $d-q$ synchronous reference frame given by

$$\begin{aligned} v_{sd} &= R_s i_{sd} + \frac{d\Psi_{sd}}{dt} - W_s\psi_{sq} \\ v_{sq} &= R_s i_{sq} + \frac{d\Psi_{sq}}{dt} + W_s\psi_{sd} \\ v_{rd} &= R_r i_{rd} + \frac{d\Psi_{rd}}{dt} - (W_s - W_r)\psi_{rq} \\ v_{rq} &= R_r i_{rq} + \frac{d\Psi_{rq}}{dt} + (W_s - W_r)\psi_{rd} \\ T_{em} &= \frac{p}{2}(\psi_{rq} i_{rd} - \psi_{rd} i_{rq}) \end{aligned} \tag{4}$$

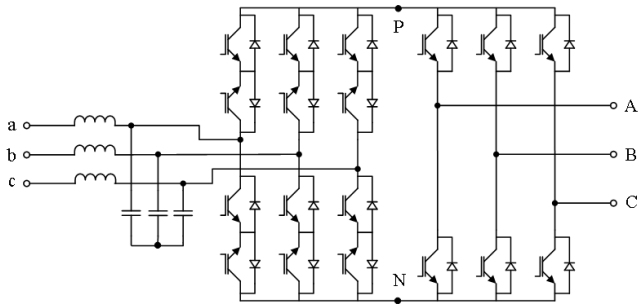

FIG. 3. Indirect matrix converter topology.

$$\begin{aligned}
\psi_{sd} &= L_s i_{sd} + L_m i_{rd} \\
\psi_{sq} &= L_s i_{sq} + L_m i_{rq} \\
\psi_{rd} &= L_m i_{sd} + L_r i_{rd} \\
\psi_{rq} &= L_m i_{sq} + L_r i_{rq} \\
L_s &= L_{ls} + L_m \\
L_r &= L_{lr} + L_m
\end{aligned} \tag{5}$$

In these equations, R_s, R_r, L_s, L_r, L_{ls}, and L_{lr} are the resistors and inductors of the stator and rotor windings, L_m is the magnetizing inductance, v_{sd}, v_{sq}, v_{rd}, v_{rq}, i_{sd}, i_{sq}, i_{rd}, i_{rq}, ψ_{sd}, ψ_{sq}, ψ_{rd}, and ψ_{rq}, are d and q components of the space vectors of the stator and rotor voltages, currents, and fluxes respectively, W_s is the synchronous speed of generator, W_r is the electrical speed of rotor, and p is the number of poles.

D. Indirect Matrix Converter

Due to the numerous advantages of matrix converters over back to back converters, in this paper the IMC is used to control the DFIG. An IMC consists of a rectification part on the input side and an inversion part on the output side, connected via fictitious dc-link as shown in Fig. 3. For purposes of analysis, we can assume that the switching frequency is far greater than the fundamental frequency of both the input voltage and output current. Thus during each switching cycle, it is assumed that both input voltage and output current are constant.

The rectifier has six bidirectional switches with the ability of conducting current and blocking voltage in both directions. The rectifier side objective is to achieve maximum positive voltages at the fictitious dc-link and sinusoidal input currents. Usually the grid side converter of DFIG exchanges zero reactive power at the grid point. In order to obtain maximum dc-link voltage, the input phase voltage which has the highest absolute value is connected to the positive or negative rail of the dc-link at 60 degree intervals depending on its polarity. To achieve sinusoidal current and unity power factor at the input side,

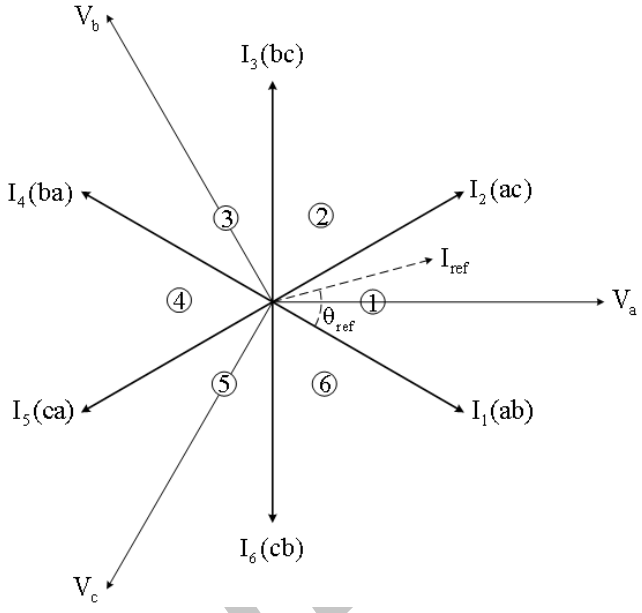

FIG. 4. Space vectors of the input current.

regardless of the load type, the other two phase voltages modulated so that the reference current space vector be in phase with the voltage space vector. Space vectors of the input current are shown in Fig. 4. Assume the input voltages are

$$\begin{aligned}
v_a &= V_m \cos\theta_a = V_m \cos(w_i t) \\
v_b &= V_m \cos\theta_b = V_m \cos(w_i t - \frac{2\pi}{3}) \\
v_c &= V_m \cos\theta_c = V_m \cos(w_i t + \frac{2\pi}{3})
\end{aligned} \tag{6}$$

where Vm is the maximum of the input phase voltage and wi is the angular frequency. In order to achieve unity power factor at the input side, the input currents must be in phase with the input voltages. Therefore, input currents are as follows

$$\begin{aligned}
I_a &= I_m \cos(w_i t) \\
I_b &= I_m \cos(w_i t - \frac{2\pi}{3}) \\
I_c &= I_m \cos(w_i t + \frac{2\pi}{3})
\end{aligned} \tag{7}$$

where Im is the maximum of the input current. On the rectifier side always two switches, one from top and another from the bottom, are ON and the others are OFF.

To calculate the duty cycle of each switch, first the angle of the input voltage space vector is obtained. This is the reference angle of the current space vector to obtain the unity power factor. Due to the angle, the section of the reference current space vector is determined from Fig. 4. Then the current reference vector can be built

using two adjacent vectors of each section. For example, when the reference current space vector is located in the first section, two adjacent vectors are ab and ac. In this section, voltage of phase a has the highest absolute value. Therefore, in 60 degree duration of this section, the top switch of phase a is ON and the bottom switches of phases b and c get modulated. Vector ab means the top switch of phase a and the bottom switch of phase b are ON, and ac means the top switch of phase a and the bottom switch of phase c are ON and so on.

So in one period of switching frequency in this section, input currents are as follows

$$\begin{aligned} i_a &= (d_{ab} + d_{ac}) i_{dc} \\ i_b &= -d_{ab} i_{dc} \\ i_c &= -d_{ac} i_{dc} \end{aligned} \tag{8}$$

where d_{ab} and d_{ac} are the duty cycles of $I_1(ab)$ and $I_1(ac)$ respectively, and i_dc is the dc-link current. As only the active vectors are used, the following relationships hold

$$d_{ab} + d_{ac} = 1 \Rightarrow i_a = i_{dc} \tag{9}$$

Therefore, the duty cycles of active vectors in the section one are given by

$$d_{ab} = -\frac{i_b}{i_a} d_{ac} = -\frac{i_c}{i_a} \tag{10}$$

The duty cycles in the other sections are obtained similarly. Based on this modulation method in the rectifier stage, the average fictitious dc-link voltage in each period is

$$\begin{aligned} V_{dc} &= \frac{3.V_m}{2.\left|\cos(\theta_{in})\right|} \\ \left|\cos(\theta_{in})\right| &= \max(\left|\cos(\theta_a)\right|, \left|\cos(\theta_b)\right|, \left|\cos(\theta_c)\right|) \end{aligned} \tag{11}$$

where θ_{in} is the angle of the input voltage space vector. On the output stage, the space vector modulation (SVM) is used to generate the required rotor voltage space vector by currents controllers. Inverter voltage space vectors along with the reference vector are shown in Fig. 5.

Duty cycles of active vectors on the inverter stage are as follow

$$d_\alpha = k.\sin(60^\circ - \theta_i) d_\beta = k.\sin(\theta_i) \tag{12}$$

where k is the modulation index and is given by

$$k = \frac{2.\left|\cos(\theta_{in})\right|.\hat{V}_r}{\sqrt{3}.V_m} \tag{13}$$

where V_r is the absolute of the reference voltage. Considering modulation of both the input and output sides, the final duty cycles of active vectors are

$$\begin{aligned} d_{\alpha\gamma} &= d_\gamma.d_\alpha d_{\beta\gamma} = d_\gamma.d_\beta \\ d_{\alpha\delta} &= d_\delta.d_\alpha d_{\beta\delta} = d_\delta.d_\beta \end{aligned} \tag{14}$$

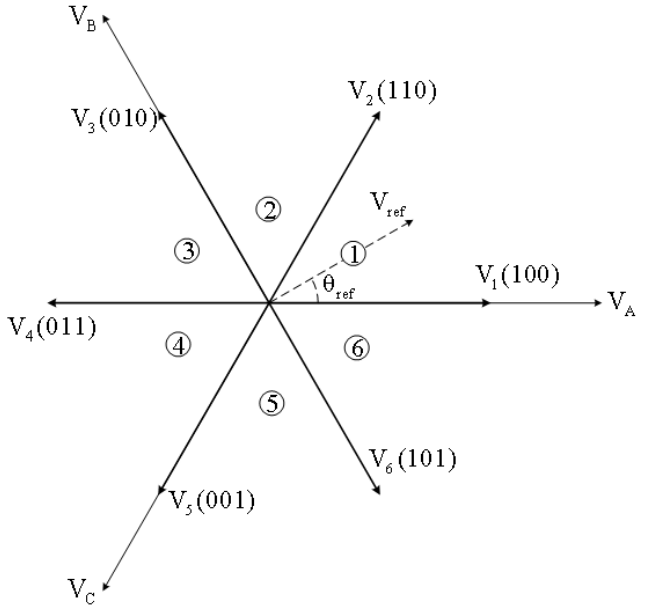

FIG. 5. Space vectors of the output voltage.

where d_γ is the first vector of the rectifier section and d_δ is the second vector of the rectifier section. Finally, the duty cycles of the zero vectors are calculated as

$$\begin{aligned} d_0 &= 1 - (d_\gamma + d_\delta).(d_\alpha + d_\beta) \\ d_{0\gamma} &= \frac{d_\gamma}{(d_\gamma + d_\delta)} d_0 d_{0\delta} = \frac{d_\delta}{(d_\gamma + d_\delta)} d_0 \end{aligned} \tag{15}$$

IV. VECTOR CONTROL OF DFIG

The goal of the DFIG controller is the independent control of the stator active and reactive power. The active power reference is determined by MPPT algorithm and the reactive power is set in order to achieve the desired power factor. Stator flux d-q reference frame is the most widely used DFIG vector control in the wind turbine applications. Thus, the inverter of IMC is controlled in a stator flux d-q reference frame, with the d-axis oriented along the stator flux vector position. For this reference frame selection, the DFIG model can be written as

$$\psi_s = \psi_{sd}, 0 = \psi_{sq} \tag{16}$$

Substituting (16) into (5), we obtain

$$
\begin{aligned}
i_{ds} &= \frac{1}{L_s}(\psi_s - L_m i_{dr}) \\
i_{qs} &= -\frac{L_m}{L_s} i_{qr} \\
\psi_{dr} &= \sigma L_r i_{dr} + \frac{L_m}{L_s}\psi_s \\
\psi_{qr} &= \sigma L_r i_{qr} \\
\sigma &= 1 - \frac{L_m^2}{L_s L_r}
\end{aligned}
\tag{17}
$$

In these equations, σ is the leakage factor. These equations are derived by assuming that the power grid is infinite, so the voltage and frequency are constant. Therefore, the dynamic of the stator flux does not need to be considered, and the stator flux is constant. These assumptions yield

$$
\frac{d\psi_{sd}}{dt} = \frac{d\psi_{sq}}{dt} = \frac{d\psi_s}{dt} = 0 \tag{18}
$$

In DFIG, the rotor voltages are control variables which control the rotor currents. Substituting (17) into (4), rotor voltages can be written as

$$
\begin{aligned}
v_{dr} &= R_r i_{dr} + \frac{d}{dt}(\sigma L_r i_{dr} + \frac{L_m}{L_s}\psi_s) \\
&\quad - (W_s - W_r)(\sigma L_r i_{qr}) \\
v_{qr} &= R_r i_{qr} + \frac{d}{dt}(\sigma L_r i_{qr}) \\
&\quad + (W_s - W_r)(\sigma L_r i_{dr} + \frac{L_m}{L_s}\psi_s)
\end{aligned}
\tag{19}
$$

In dynamic performance analysis of the overall system, cross-coupling terms in (19) are added to control loops as feed-forward compensation terms. The stator active and reactive power can be calculated as

$$
\begin{aligned}
P_s &= \frac{3}{2}(v_{ds} i_{ds} + v_{qs} i_{qs}) \\
Q_s &= \frac{3}{2}(v_{qs} i_{ds} - v_{ds} i_{qs})
\end{aligned}
\tag{20}
$$

In steady state, the stator flux is proportional to the grid voltage. Neglecting the small voltage drop in the stator resistance yields

$$
\begin{aligned}
V_s = v_{qs}, 0 = v_{ds} \\
|Vs| \simeq w_s |\psi_s|
\end{aligned}
\tag{21}
$$

Thus, when orienting the d-axis with the stator flux, the voltage aligns with the q-axis. Combining (21) and (16)

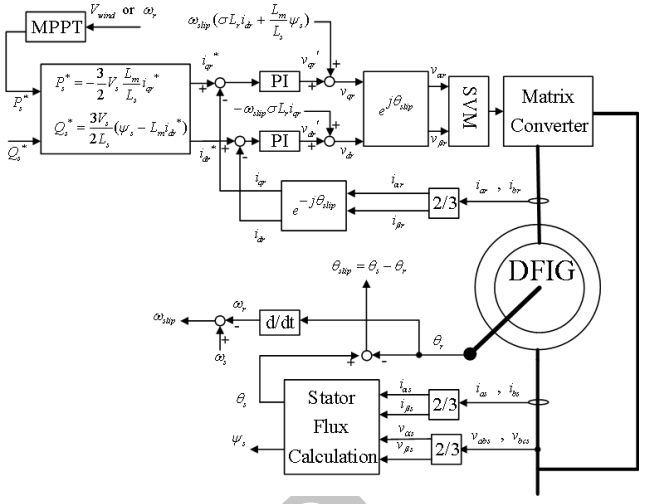

FIG. 6. Schematic diagram of vector control of DFIG.

with (20), we obtain

$$
\begin{aligned}
P_s &= \frac{3}{2} v_{ds} i_{ds} = -\frac{3}{2} V_s \frac{L_m}{L_s} i_{qr} \\
Q_s &= \frac{3}{2} v_{qs} i_{ds} = \frac{3V_s}{2L_s}(\psi_s - L_m i_{dr})
\end{aligned}
\tag{22}
$$

The above equations clearly show that under the stator flux orientation, the active and reactive powers are decoupled and can be controlled via the rotor currents. By means of i_{qr}, we can control the active power while the reactive power can be controlled via the i_{dr}. Using the above equations, the reference currents can be calculated from the desired powers. The schematic diagram of stator flux based vector control of DFIG is shown in Fig. 6.

V. ADAPTIVE CONTROL

Traditionally, the controllers are proportional-integral (PI) types and tuning their parameters is based on assuming the stator voltage to be ideal. Therefore, the rate of change of stator flux linkage in (4) is often neglected which is equivalent to neglect the stator electric transients. Considering the cross-coupling terms as feed-forward compensation terms in controller loops, the DFIG model can be simplified to a first order model in d-q axis. The controller based on this first-order model works well in normal operating conditions. But, in fault conditions and the DFIG terminal voltage drops such assumption is not valid. For more precise modeling of a DFIG in fault situations, the derivative terms of stator flux linkage should be taken into account. Therefore, by applying the stator flux derivatives into the rotor voltage

equations, (19) is modified as below

$$v_{rd} = R_r i_{rd} + L_{\sigma r}\frac{di_{rd}}{dt} - w_{slip}L_{\sigma r}i_{rq} - w_{slip}\frac{L_m}{L_s}\psi_{sq} + \frac{L_m}{L_s}\frac{d\psi_{sd}}{dt}$$
$$v_{rq} = R_r i_{rq} + L_{\sigma r}\frac{di_{rq}}{dt} + w_{slip}L_{\sigma r}i_{rd} + w_{slip}\frac{L_m}{L_s}\psi_{sd} + \frac{L_m}{L_s}\frac{d\psi_{sq}}{dt} \quad (23)$$

By combining (5) and (23) one can conclude that considering the derivatives of the stator flux linkage in fault conditions, the dynamic model of the DFIG will be modified. As a result, in fault conditions the PI parameters should be altered. Therefore, in our proposed method two sets of PI parameters are designed and tuned specifically for normal and fault conditions and stored in a look up table. The default PI parameters are for normal operation. On the occurrence of a fault the parameters of PI controller is updated via look-up table. The block diagram of the proposed control scheme is depicted in Fig. 7. The proposed control system can adapt itself to changes of DFIG dynamics and achieve a good dynamic performance in both normal and fault conditions.

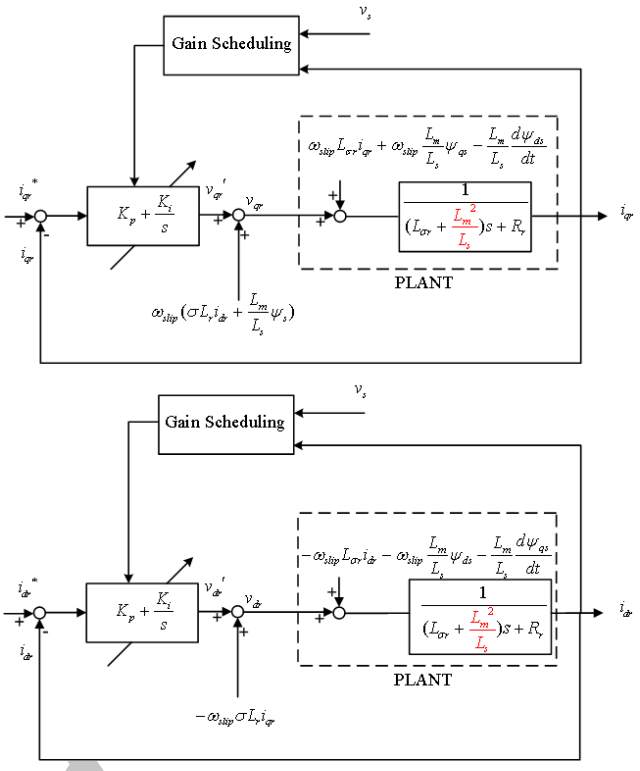

FIG. 7. Block diagram of proposed control scheme simulation results.

A. Normal Operation

Simulations are carried out in PSIM environment to investigate the effects of switching. However, the outputs from PSIM are sent to MATLAB for presenting more clear graphical results. The studied system is a 1.5 MW wind turbine. The wind turbine, gearbox, and DFIG parameters are provided in Appendix. To analyze the dynamic performance and MPPT algorithm for extracting the maximum power at any wind speed, the DFIG wind turbine excited by indirect matrix converter in normal operation mode is simulated. The simulation result presented in Fig. 8. To investigate the performance of MPPT algorithm and change of the active power reference, it is assumed the wind turbine moment of inertia to be 10% of its real value for reducing the simulation time. Total simulation time in this part is 3 seconds. Wind speed is considered as variable and at $t = 1.6$ s has been reduced to 6 m/s. Speed starts to reduce due to a sharp reduction in turbine mechanical torque as shown in Fig. 8a The stator active power with the reference value is shown in Fig. 8b. One of the advantages of the DFIG wind turbine is the independent control of active and reactive power. Referring to (22) the stator reactive power corresponds to d-axis component of the rotor current. Fig. 8c shows the d-axis component of the rotor current with its reference value. At $t = 1$ s reactive power reference value is changed to 0.6 pu and at $t = 2$ s is set to zero. Fig. 8c shows that the d-axis component of the rotor current well tracks the reference value and controller renders a good dynamic performance in normal operation. The rectifier of indirect matrix converter is controlled so that the input voltage and current are in phase. Fig. 8d shows the stator and rotor currents of phase a. As can be seen from this figure the frequency of the rotor current is proportional to slip and becomes dc-current around synchronous speed.

B. Fault Condition

In this section performance of a DFIG wind turbine is simulated under fault conditions. As was mentioned in section II according to FRT standard of Germany, wind turbines must remain connected to grid following occurrence of grid faults. Moreover, they must also inject reactive power to help the grid for voltage recovery. To simulate the fault condition, at $t = 0.7$ s the grid voltages are dropped by 50% for 300 ms as shown in Fig. 9. Fig. 10 shows the rotor currents in this case while controller is designed for normal operation without any protection. For such voltage sag, the rotor currents are increased to 1.6 pu. In the absence of any protecting device, these high currents can destroy the IGBT switches of the IMC. Fig. 11 shows the rotor currents when the proposed adaptive control system is in operation. Crowbar activation signal is obtained from comparison of rotor currents with a threshold value defined by the maximum sustainable current of IGBT switches. In this simulation

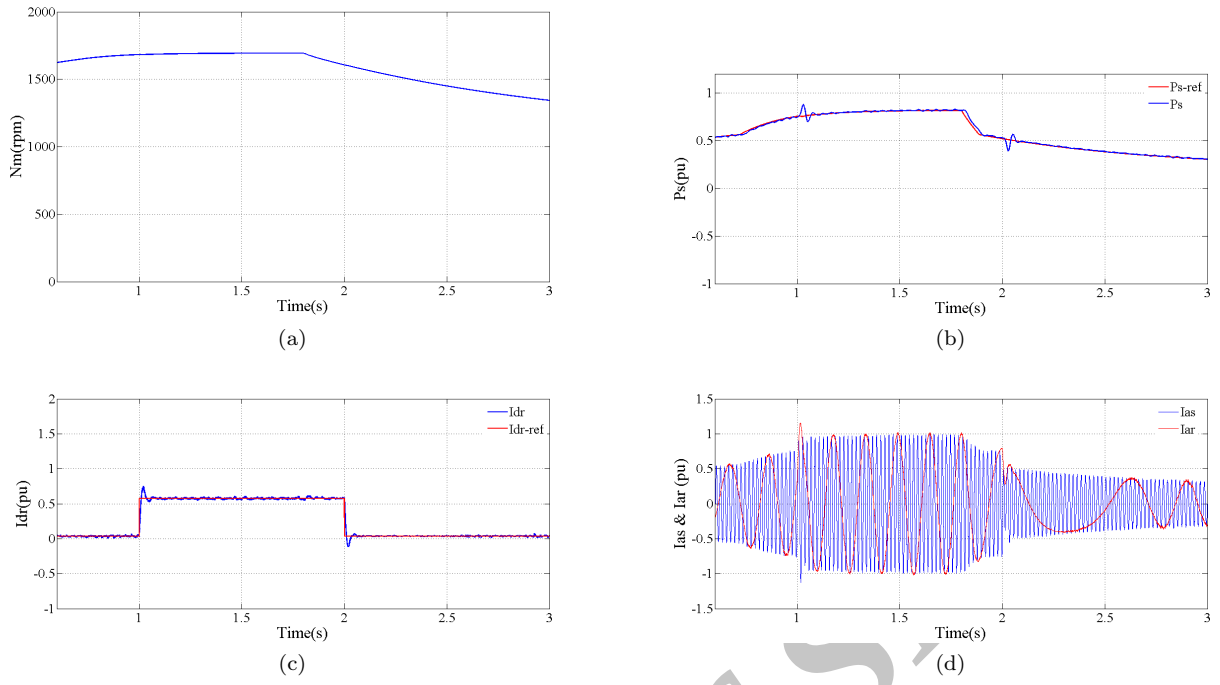

FIG. 8. Simulation of DFIG wind turbine excited by IMC in normal operation mode: **(a)** rotor speed, **(b)** active power, **(c)** rotor d-axis current and **(d)** stator and rotor currents.

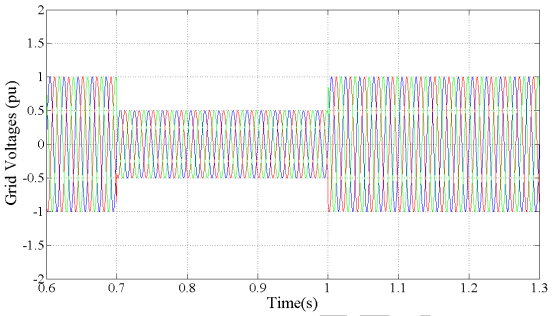

FIG. 9. Grid voltages.

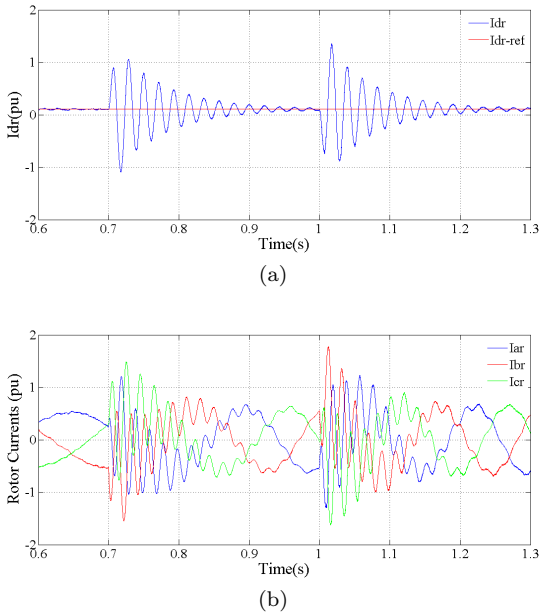

FIG. 10. Rotor currents in fault condition, with the controller designed for normal operation: **(a)** rotor d-axis current and **(b)** rotor three phase currents.

the threshold value is set to 1.4 pu. When the rotor current is greater than the threshold value, the crowbar is activated.

Therefore, as shown in Fig. 11 the rotor fault currents are always in the safe operating area of IGBT switches. The proposed adaptive controller, in compare with conventional PI controller, provides rapid currents damping. For the studied system the settling time reduces from 200 ms to 100 ms and makes it possible to inject reactive power more quickly as required by new FRT standards. Crowbar activation signal presented in Fig. 11c, shows that crowbar will instantly be activated if the rotor currents exceed the threshold value. In contrast to conventional PI controller, in the proposed controller the crowbar is active for a shorter time, so for most of the time during fault, the control system of DFIG is in operation injecting reactive power to grid. In order to meet the new FRT standards, during fault the references of the active and reactive powers are set as 0.0 pu and 1.0

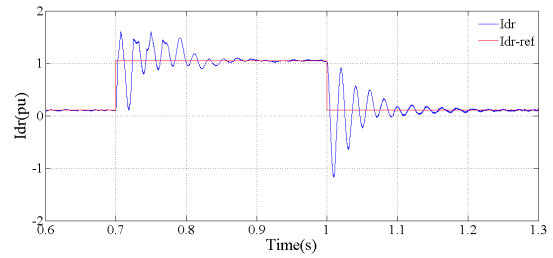

(a)

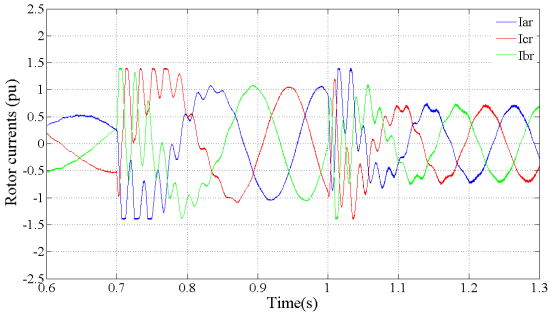

(b)

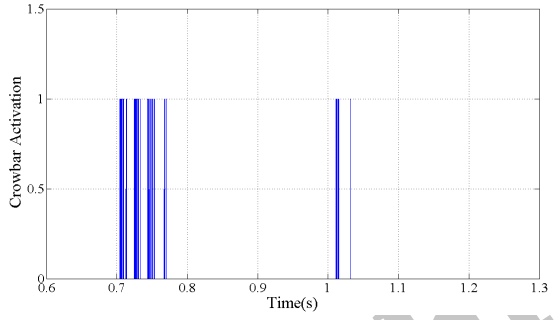

(c)

FIG. 11. Rotor currents in fault condition, with the proposed method: **(a)** rotor d-axis current, **(b)** rotor three phase currents and **(c)** crowbar activation signal.

pu, respectively. As can be seen from Fig. 11, injection of 1.0 pu reactive current is realized in comply with FRT standard.

VI. CONCLUSIONS

To enhance the LVRT capability of DFIG wind turbines based on indirect matrix converters (IMCs), in this paper a new method is proposed. This method consists of an adaptive gain scheduling controller instead of conventional PI controller. In this approach not only the IMC is protected against large fault currents but the rapid currents damping is also provided. The activation time of crowbar is considerably reduced so, the control system can be in operation most of the fault duration. Therefore, the immediate reactive power injection is realized to help voltage recovery in order to satisfy the new FRT standards. Simulation results confirm the efficiency of the proposed method.

APPENDIX

Parameters of the studied system are as follows.

Wind turbine:

$$P_{nom} = 1.5\ MW$$

$$Base\ Wind\ Speed = 12\ m/s$$

$$Moment\ of\ inertia = 1.2\ Mkg.m^2$$

Gearbox:

$$n_1/n_2 = 1/100$$

DFIG:

$$P_{nom} = 1.5\ MW,\ V_{nom} = 690\ V$$

$$f_{nom} = 50\ Hz,\ R_s = 10.3\ m\Omega$$

$$R_r = 8.28\ m\Omega,\ L_{ls} = 0.2801\ mH$$

$$L_{lr} = 0.1177\ mH,\ L_m = 26.96\ mH$$

$$P = 6,\ J = 116\ Kg.m^2$$

REFERENCES

[1] "World Wind Energy Report 2010," *Report. World Wind Energy Association. [Online]. Available: http://www.wwindea.org*, Aprill 2011.

[2] L. H. Hansen, L. Helle, F. Blaabjerg, E. Ritchie, S. Munk-Nielsen, H. Bindner, P. Sorensen and B. Bak-Jensen, "Conceptual survey of Generators and Power Electronics for Wind Turbines," *Riso National Laboratory, Roskilde, Denmark*, December 2001.

[3] L. Wei and T. A. Lipo, "A novel matrix converter topology with simple commutation," *Industry Applications Conference, 2001. Thirty-Sixth IAS Annual Meeting. Conference Record of the 2001 IEEE*, pp.1749-1754 Sept. 30 2001-Oct. 4 2001.

[4] G. Michalke, "Variable Speed Wind Turbines- Modeling, Control, and Impact on Power Systems," PhD Thesis, *Riso National Laboratory*, 2008.

[5] Z. Cheng and Y. Gangui, "Study on transient performance of doubly fed induction generator with crowbar during three-phase voltage dips," *2015 9th International Conference on Power Electronics and ECCE Asia (ICPE-ECCE Asia), Seoul*, pp. 373-376, 2015.

[6] S. Yang, T. Zhou, X. Zhen, X. Zhang, R. Shao and L. Chang, "A SCR crowbar commutated with rotor-side converter for doubly fed wind turbines," *2015 IEEE 6th International Symposium on Power Electronics for Distributed Generation Systems (PEDG), Aachen*, pp. 1-7, 2015.

[7] M. A. Chowdhury, A. H. M. Sayem, W. Shen and K. S. Islam, "Robust active disturbance rejection controller design to improve low-voltage ride-through capability of doubly fed induction generator wind farms," in *IET Renewable Power Generation*, vol. 9, no. 8, pp. 961-969, 2015.

[8]Z. Wei, Z. Peng and H. Yikang, "Analysis of the by-pass resistance of an active crowbar for doubly-fed induction generator based wind turbines under grid faults," *Electrical Machines and Systems, 2008. ICEMS 2008. International Conference on*, pp. 2316-2321, 17-20 Oct. 2008.

[9]A. Khajeh and R. Ghazi, "Control of DFIG Wind Turbines Based on Indirect Matrix Converters in Short Circuit Mode to Improve the LVRT Capability," *Advances in Power Electronics*, Article ID 157431, 11 pages, 2013.

[10]B. I. Nss, M. Molinas and T. Undeland, "Laboratory tests of ride through for doubly fed induction generators," *In NWPC, Espoo, Finland*, May, 2006.

[11]G. Tsourakis and C.D. Vournas, "Simulation of low voltage ride through capability of wind turbines with double fed induction generator," *In EWEC, Athens, Greece*, March 2006.

[12]M. A. Chowdhury, A. H. M. Sayem, W. Shen and K. S. Islam, "Robust active disturbance rejection controller design to improve low-voltage ride-through capability of doubly fed induction generator wind farms,"in *IET Renewable Power Generation*, vol. 9, no. 8, pp. 961-969, 2015.

[13]Q. Huang, X. Zou, D. Zhu and Y. Kang, "Scaled Current Tracking Control for Doubly Fed Induction Generator to Ride-Through Serious Grid Faults,"in *IEEE Transactions on Power Electronics*, vol. 31, , no. 3, pp. 2150-2165, March 2016.

[14]R. Ghazi and A. Khajeh, "GA-Based Optimal LQR Controller to Improve LVRT Capability of DFIG Wind Turbines," *IJEEE*, Vol. 9, No. 3, pp. 167-176, 2013.

[15]F. K. A.Lima, A. Luna, P. Rodriguez, E. H. Watanabe and F. Blaabjerg, "Rotor Voltage Dynamics in the Doubly Fed Induction Generator During Grid Faults," *Power Electronics, IEEE Transactions on*, vol. 25, no. 1, pp. 118-130, Jan 2010.

[16]L. Jiaqi, Q. Wei and R. G. Harley, "Direct transient control of wind turbine driven DFIG for low voltage ride-through," *Power Electronics and Machines in Wind Applications, 2009. PEMWA 2009. IEEE*, pp. 1-7, 24-26 June 2009.

[17]M. R. Rathi and N. Mohan, "A novel robust low voltage and fault ride through for wind turbine application operating in weak grids," *Industrial Electronics Society, 2005. IECON 2005. 31th Annual Conference of IEEE*, pp., 6-10 Nov. 2005.

[18]O. Gomis-Bellmunt, A. Junyent-Ferre, A. Sumper and J. Bergas-Jan, "Ride-Through Control of a Doubly Fed Induction Generator Under Unbalanced Voltage Sags," *Energy Conversion, IEEE Transactions on*, vol. 23, no. 4, pp. 1036-1045, Dec. 2008.

[19]Z. Yi, P. Bauer, J. A. Ferreira and J. Pierik, "Operation of Grid-Connected DFIG Under Unbalanced Grid Voltage Condition," *Energy Conversion, IEEE Transactions on*, vol. 24, no. 1, pp. 240-246, March 2009.

[20]D. Li and H. Zhang, "A combined protection and control strategy to enhance the LVRT capability of a wind turbine driven by DFIG," *Power Electronics for Distributed Generation Systems (PEDG), 2010 2nd IEEE International Symposium on*, pp. 703-707, 16-18 June 2010.

[21]C. Abbey and G. Joos, "Short-term energy storage for wind energy applications," *Industry Applications Conference, 2005. Fourtieth IAS Annual Meeting. Conference Record of the 2005*, pp. 2035-2042, 2-6 Oct. 2005.

[22]C. Abbey, Li. Wei, L. Owatta and G. Joos, "Power Electronic Converter Control Techniques for Improved Low Voltage Ride Through Performance in WTGs," *Power Electronics Specialists Conference, 2006. PESC '06. 37th IEEE*, pp. 1-6, 18-22 June 2006.

[23]I. Erlich, H. Wrede and C. Feltes, "Dynamic Behavior of DFIG-Based Wind Turbines during Grid Faults," *Power Conversion Conference - Nagoya, 2007. PCC '07*, pp. 1195-1200, 2-5 April 2007.

[24]J. Amini, R. Kazemzahed and H. Madadi Kojabadi, "Performance enhancement of indirect matrix converter based variable speed Doubly-Fed induction generator," *Power Electronic & Drive Systems & Technologies Conference (PEDSTC), 2010 1st*, pp. 450-455, 17-18 Feb. 2010.

[25]E. Reyes, R. Pena, R. Cardenas, J. Clare and P. Wheeler, "Control of a Doubly-fed Induction Generator with an Indirect Matrix Converter with changing DC voltage," *Industrial Electronics (ISIE), 2010 IEEE International Symposium on*, pp. 1230-1235, 4-7 July 2010.

[26]D. Wenlang, C. Zhiyong, Z. Liming and Y. Yu, "Research on the performance of low voltage ride-through for doubly fed induction generator excited by two-stage matrix converter," *Power Electronics and Motion Control Conference, 2009. IPEMC '09. IEEE 6th International*, pp. 638-643, 17-20 May 2009.

Ahmad Khajeh was born in Zabol, Iran in 1982. He received the B.Eng. degree from Sistan and Baluchestan Universtity, Zahedan, Iran, in 2004, and the M.Eng. and Ph.D. degrees from Amirkabir University of Technology and Ferdowsi University of Mashhad, Iran, in 2007 and 2014, all in electrical engineering, respectively. Currently, he is an Assistant Professor with the Faculty of Electrical and Computer Engineering, University of Sistan and Baluchestan, Zahedan, Iran. His current research interests include power electronics, wind power, adjustable speed drives and photovoltaic system.

Zahra Shabani was born in Langroud, Iran in 1984. He received the B.Sc. degree from Bu-Ali Sina University, Hamedan, Iran, in 2006, and the M.Sc. and Ph.D. degrees from Ferdowsi University of Mashhad, Iran, in 2008 and 2013, all in Mathematics, respectively. Currently, she is an Assistant Professor with the Department of Mathematics, Faculty of Mathematics, University of Sistan and Baluchestan, Zahedan, Iran. Her current research interests include Dynamical Systems, Ergodic Theory and Chaos.